Australia's National Science Agency

GISERA | Gas Industry Social and Environmental Research Alliance

Baseline Seismicity of Beetaloo Basin-Final Report

April 2025

Citation

Saygin, E, Qashqai MT and Guo, P (2025) Baseline Seismicity of Beetaloo Basin, Final Report. CSIRO, Australia.

Copyright

© Commonwealth Scientific and Industrial Research Organisation 2023. To the extent permitted by law, all rights are reserved and no part of this publication covered by copyright may be reproduced or copied in any form or by any means except with the written permission of CSIRO.

Important disclaimer

CSIRO advises that the information contained in this publication comprises general statements based on scientific research. The reader is advised and needs to be aware that such information may be incomplete or unable to be used in any specific situation. No reliance or actions must therefore be made on that information without seeking prior expert professional, scientific and technical advice. To the extent permitted by law, CSIRO (including its employees and consultants) excludes all liability to any person for any consequences, including but not limited to all losses, damages, costs, expenses and any other compensation, arising directly or indirectly from using this publication (in part or in whole) and any information or material contained in it.

CSIRO is committed to providing web accessible content wherever possible. If you are having difficulties with accessing this document please contact csiro.au/contact

Table of Contents

Figures

Tables

Acknowledgement

This research has been funded through CSIRO's Gas Industry Social and Environmental Research Alliance (GISERA) with contributions from the Australian Government's Department of Industry, Science, and Resources. GISERA is a collaboration between CSIRO, Commonwealth, state and territory governments and industry established to undertake research on the impacts of onshore gas exploration and development on the environment, and the socio-economic costs and benefits. For information about GISERA's governance structure, projects and research findings visit https://gisera.csiro.au.

The authors of this report also acknowledges Dr Cameron Huddlestone-Holmes (CSIRO) for championing this project, Prof. Brian L.N. Kennett (The Australian National University) on discussions about the historical seismicity in the Northern Territory and Dr Trevor Allen (Geoscience Australia) for making the first phase seismic data available.

Executive Summary

The Beetaloo sub-basin is one of the largest basins in the Northern Territory, with proven significant shale gas potential. Over the years, the importance of the Beetaloo sub-basin has increased with the planned subsurface resource-based projects. In the case of prospective unconventional resource development activities, it is expected that hydraulic fracturing technologies will be used. A monitoring plan is needed to distinguish between hydraulic fracturing-induced and baseline seismicity (natural earthquakes). The Scientific Inquiry into Hydraulic Fracturing in the Northern Territory stated that “Australia does not yet have any seismic risk data covering shale gas operations or a national record of seismicity below magnitude 4 on the Richter scale”. Although natural earthquake activity in the Australian continent is relatively low compared to its neighbours such as Indonesia and its surroundings, large magnitude earthquakes can occur in the continent with very long recurrence rates, making earthquake risk calculations difficult with large uncertainties. For example, in 1988, three consecutive large earthquakes occurred in the south of the Beetaloo sub-basin. Prior to these events, only moderate seismicity was observed in 1987, and no other significant seismic activity was recorded in the recorded history.

In this project, we used a continuous seismic dataset recorded by sparsely distributed regional seismic sensor array deployed by Geoscience Australia to investigate the baseline seismic activity levels within the Beetaloo sub-basin and its nearby surroundings. Detection of small-sized earthquakes is an arduous task as the signal can be buried within environmental noise that also affects the sensitivity of sensors. We investigated the relative noise levels as well as environmental noise sources. For earthquake detection and location, we ran state-of-the-art machine-learning based methods to detect and locate any seismic activity. Apart from the mining blasts approximately 200 km away from the seismic array, we did not detect any natural seismic activity within the region for the years between 2019 and 2024. However, we stress that the lack of seismic activity can be a function of the sparse seismic array, which affects the detection threshold, or a real lack of seismicity. In the project, for the first time in Australia, we also trialled a physics-based simulation method to estimate the ground shaking at any point within the basin caused by a hypothetical but a realistic earthquake scenario in the region.

Finaly, we argue that with the relatively long recurrence rates of large magnitude earthquake activity across Australia, it is paramount to continue seismic monitoring with a tightly clustered network, to properly quantify the seismic risk. We also propose to examine the surface imprints of previous large earthquake activity in the region by analysing satellite-derived digital elevation models. By coupling these two classes of information, the natural seismic risk of the region, which is still enigmatic, can be resolved.

Background

Hydraulic fracturing is a key enabling technology that helped unlock vast reserves of unconventional oil and gas resources within low permeability hydrocarbon rocks globally. The production takes place by injecting high pressure engineered fluids to create a permeable pathway for fluid flow in the subsurface. The injected fluids are generally disposed of at other wells for long term storage. It has been clearly demonstrated that (see Atkinson et al., 2020 for a comprehensive review) there is a correlation between hydraulic fracturing & injected water volumes and induced earthquake activity often in the vicinity of the production sites. Hydraulic fracturing is expected to create weak seismicity during opening of existing fractures to enhance permeability of the reservoir (also called operationally induced seismicity) (Atkinson et al., 2020). Larger and damaging earthquakes may occur if wastewater injection volumes are large enough, as in central Oklahoma in September 2016 (Pawnee event), where a magnitude 5.8 earthquake caused building damage. Hydraulic fracturing itself can trigger earthquakes in critically stressed faults as in the magnitude 5.7 event in Sichuan Basin, China. However, it must be noted that the lack of depleted reservoirs in the Northern Territory removes the possibility of large volumes of waste-water injection.

Beetaloo Sub-Basin is an onshore basin located in the Northern Territory, Australia, with a proven significant shale gas potential. In the case of prospective unconventional resource development activities, it is expected that hydraulic fracturing technologies will be used. A seismic monitoring plan is needed to distinguish between induced and baseline seismicity (natural earthquakes). Around the world, several seismic networks have been deployed and operated before, during and after the resource development operations. A good example is U.S. TexNet array, in which several seismographs are operated to provide real-time information about the seismic activity. In Australia, the Kimberley array has been deployed by the Geological Survey of Western Australia. CSIRO Scientists are analysing data from this array to quantify the baseline seismicity. Since late 2019, Geoscience Australia has been operating a six-element seismic broadband array in the Beetaloo Basin. The data is real-time telemetered to Geoscience Australia and freely open to the public (Figure 1D, blue triangles).

Outline

In this final report, we merged the outputs of two previous interim reports and also present the final work on optimal station design and potential future studies.

We first identified the potential sources of seismic activity by mapping the available spatial data. We then assessed the quality of the seismic stations operated by Geoscience Australia (Beetaloo Seismic Network – 2O) by analysing quarterly seismic noise variations, which is one of the parameters that determines the detection sensitivity of a seismic station. Next, we examined the waveforms recorded across the network for local, regional, and distant earthquakes. Using a state-of-the-art method, we detected only man-made seismic activity within the region for 5 years. We also present examples of ground motion simulations using a continent-scale seismic velocity model, a first in Australia. In these simulations, we estimated the potential shaking in the future using parameters from a real earthquake that occurred in the nearby town of Tennant Creek. Despite being a very high-quality seismic network, the sensor spacing is above 50 km. We argue that with this spacing, it is not possible to detect small seismic activity ($M < 2$) if it exists within the basin.

Finally, we provide future perspectives on the optimum seismic network design to increase the success of small magnitude earthquake detection and systematically study surface features to explore surface rupture from any historical seismicity prior to the seismic instrumentation era. For this, we propose a systematic study of satellite-derived digital elevation models with machine learning-based automated techniques to discover them to fully quantify the seismic risk within the basin.

Potential Sources of Seismic Activity

In this section, we first mapped the location of major roads, active mine sites, petroleum wells as well as the current seismic network in Figure 1 to estimate the potential seismic source locations including anthropogenic sources such as vehicle noise from the road network (Figure 1A) and mine blasting (Figure 1B). The region is sparsely populated hence it is not expected to observe much traffic noise recorded by the seismic stations (Figure 1D). The large mining projects in the region to the north and south of the network generate observable seismic noise, where regular day time blasting by active mine sites in the area generates observable seismic signals, as has been previously reported by Geoscience Australia (Shamsalsadati et al., 2021).

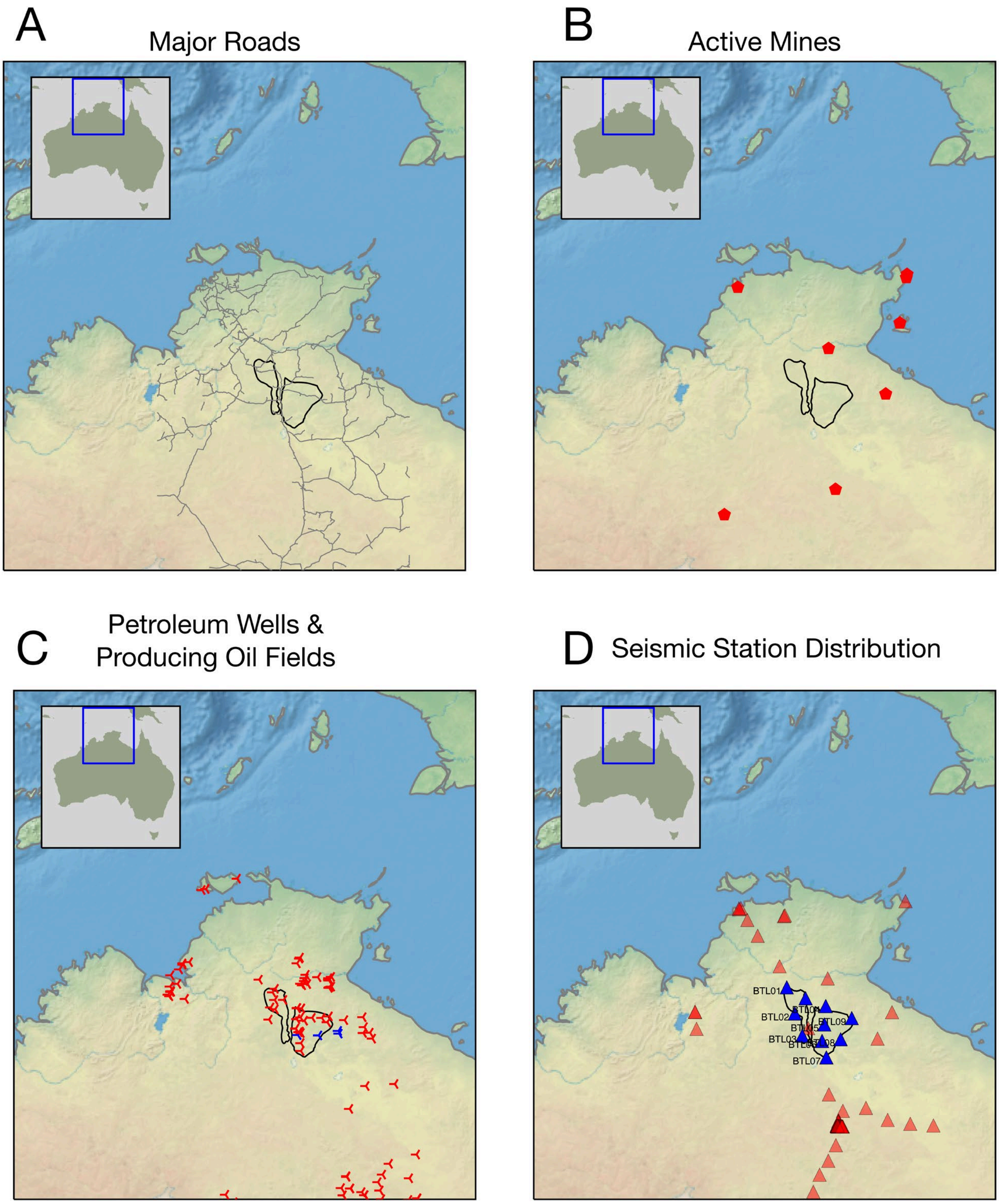

Figure 1 A) Location of major roads in the region, B) Distribution of active mine sites, C) Distribution of Petroleum wells (red) and producing oil fields (blue), D The distribution of current and past passive seismic stations. Red triangles show previous deployments, and blue triangles show the Beetaloo Seismic Network with station codes. The outline of the Beetaloo Basin is given with black line in each panel.

Performance of the Beetaloo Seismic Network

One common approach to quantifying the detection performance of seismic stations in the presence of surrounding noise, such as human activity and ocean-generated noise, is to conduct seismic noise analyses using continuous seismic records. These records capture various environmental sources, including ocean-ground interactions, anthropogenic sources (human-made), and very large earthquakes. Notably, the standing waves induced by storms in the ocean create a distinctive seismic signature in the frequency range of 0.09 – 0.18 Hz (Kennett, 2001). The level of noise variability also changes with seasonal variations in storm activity. Additionally, mid-continental stations generally exhibit lower noise levels, making them more sensitive to earthquake signals. Analysing these signals offers a metric for quantifying the theoretical performance of a seismic network (McNamara & Buland, 2004)

Background Seismic Noise Recorded at Beetaloo Seismic Network

We compute the probability density functions of seismic signals recorded at each station across the Beetaloo Basin Network to evaluate the range of variation of seismic noise in time and frequency. In the data processing, we remove the instrument response and digitiser gain to minimize the contribution of the instruments. The processing stream divides each record into one-hour-long segments with a 50% overlapping window. Then, we calculate the amplitude spectrum of each data segment and average them out to create the probabilistic density spectrum. We present the average variation of seismic noise levels as a function of frequency and time for three different seismic stations. Figures 2-4 provide quarterly changes in results for BTL01 (north of the basin), BTL05 (centre), and BTL07 (south of the basin).

Overall, the seismic noise levels are close to the 'New Low Seismic Noise Model' (McNamara & Buland, 2004) even at higher frequencies, indicating that the stations are located in quiet zones, which offer higher sensitivity to weak seismic activity, such as smaller magnitude earthquakes. Seismic noise generated by atmosphere-ocean-ground interactions, such as distant storms, often exhibits strong seasonality and slight interannual variability in Australia, as documented by Reading et al. (2014). However, in the case of the Beetaloo Seismic Network, we observed very little variation, as demonstrated by the computed probabilistic spectral density functions for the entire network.

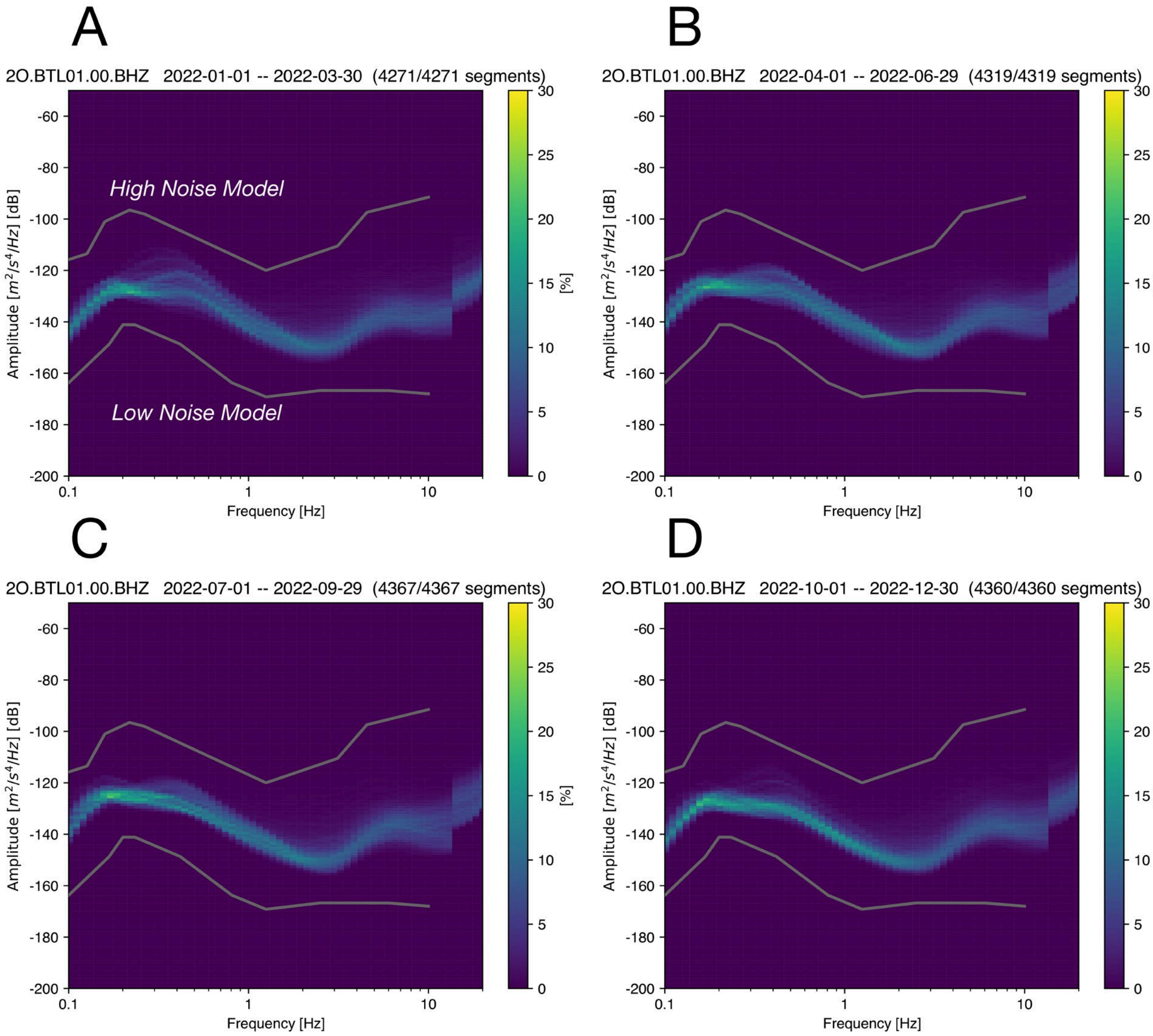

Figure 2 A) The background seismic noise variations for BTL01 (north) between January and March 2022 for signals between 0.1 and 50 Hz. B) April 2022 and June 2022. C) July 2022 and September 2022. D) October 2022 and December 2022. Although distant storm activities were expected to cause changes in lower frequencies (< 2 Hz), the observed signals remained close to the low noise model (as marked in A). The higher frequency signals were not greatly affected by expected anthropogenic activities.

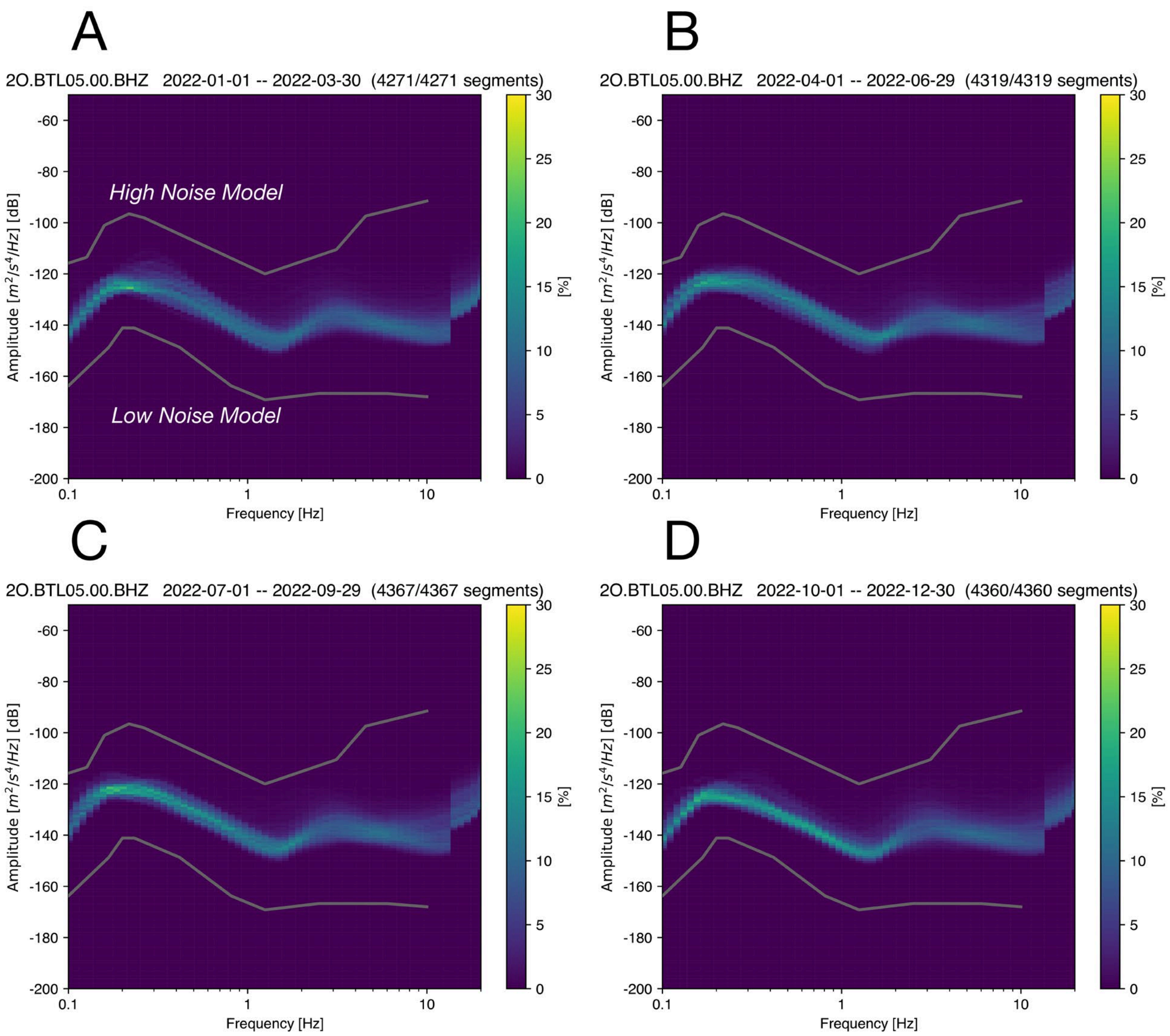

Figure 3: A) The background seismic noise variations for BTL05 (centre) between January and March 2022 for signals between 0.1 and 50 Hz. B) April 2022 and June 2022. C) July 2022 and September 2022. D) October 2022 and December 2022. Although distant storm activities were expected to cause changes in lower frequencies (< 2 Hz), the observed signals remained close to the low noise model (as marked in A). The higher frequency signals were not greatly affected by expected anthropogenic activities.

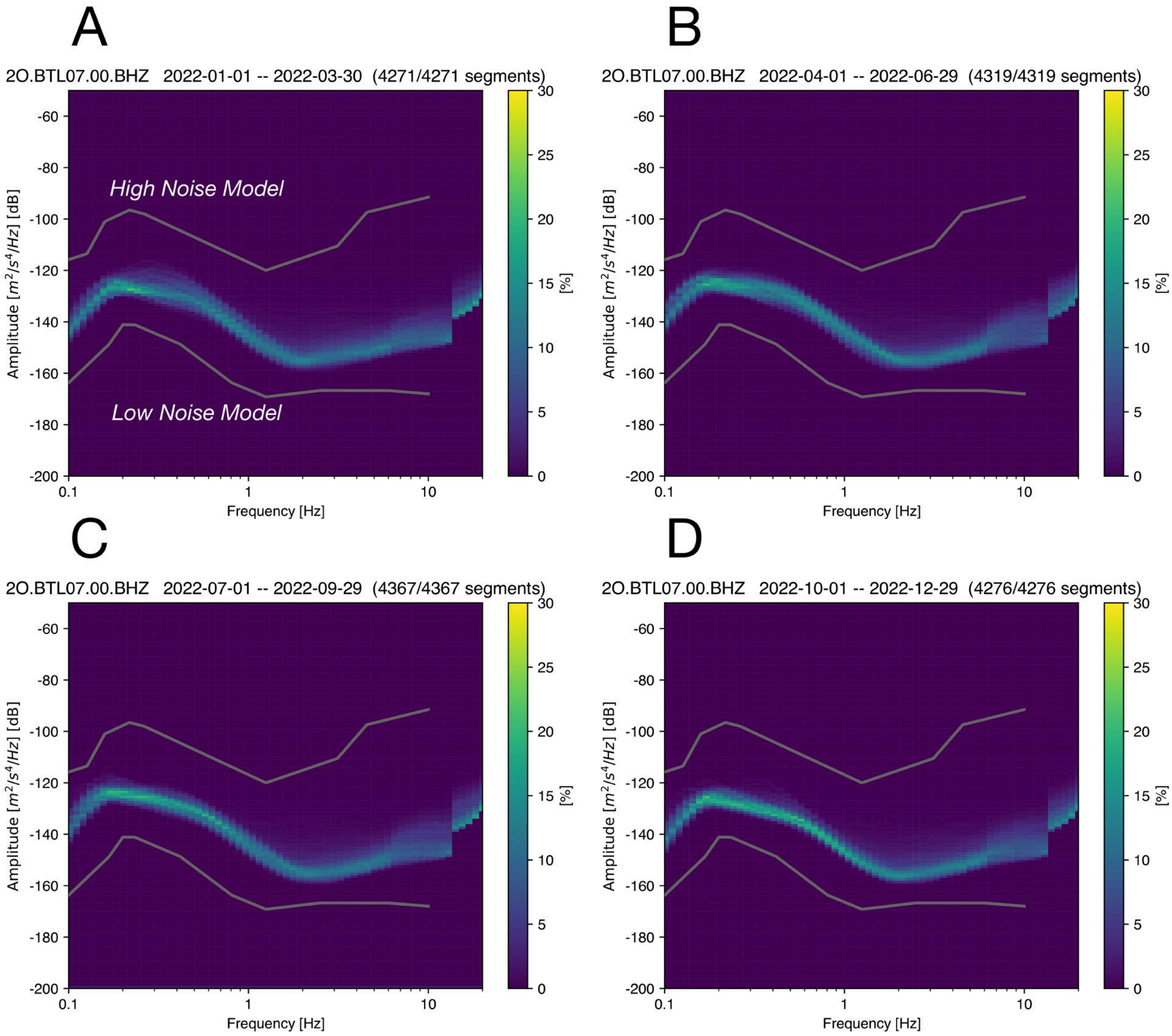

Figure 4: A) The background seismic noise variations for BTL07 (south) between January and March 2022 for signals between 0.1 and 50 Hz. B) April 2022 and June 2022. C) July 2022 and September 2022. D) October 2022 and December 2022. Although distant storm activities were expected to cause changes in lower frequencies (< 2 Hz), the observed signals remained close to the low noise model (as marked in A). The higher frequency signals were not greatly affected by expected anthropogenic activities.

Example Recordings of Distant Earthquakes

Another method to assess the performance of a seismic network involves examining recordings of moderate to large magnitude regional and distant earthquakes catalogued by other agencies, such as the USGS. Various factors, including environmental noise, installation procedures, instrumentation, and site conditions, collectively influence the quality of the recorded signals, which subsequently affects the baseline seismic characterization efforts.

For our analysis, we selected three distinct earthquakes occurred in 2022, originating from Australia, Indonesia, and Mexico, respectively, each with different magnitudes. Figure 5 depicts the event locations and seismic station placements. Notably, despite a wide range of distances between the earthquakes and stations (~300 km – 14,000 km), the seismic events were captured with high fidelity across all three components (vertical, north-south, and east-west) of the stations, as shown in Figure

6. For instance, the wavefield resulting from the regional earthquake with a magnitude of 4.4 is clearly visible throughout the network (Figure 6C), indicating the interaction between the waves and the relatively shallow structure with high-frequency wave propagation. Conversely, the far-field earthquake originating from Mexico (Figure 6A) exhibits relatively weaker waves originating from the deep layers of the Earth. Here, the Earth acts as filter, leading to the attenuation of most high-frequency waves.

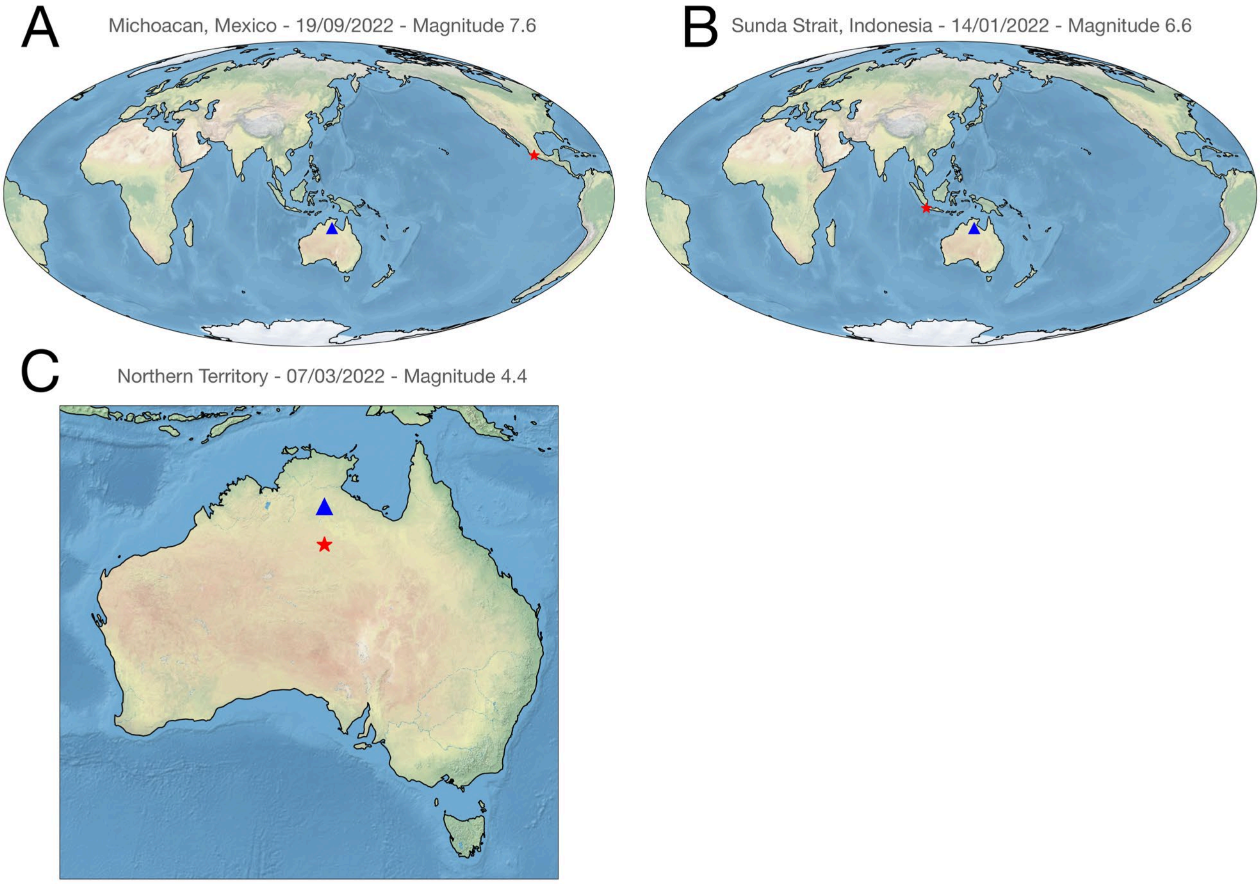

Figure 5: The location of three different earthquakes (red stars) recorded by the Beetaloo Basin seismic network (blue triangle). The average distances between earthquakes and the network stations are A) 14,000 km, B) 3200 km and C) 300 km. Titles of each sub plot show the location, date, and the magnitude of each event.

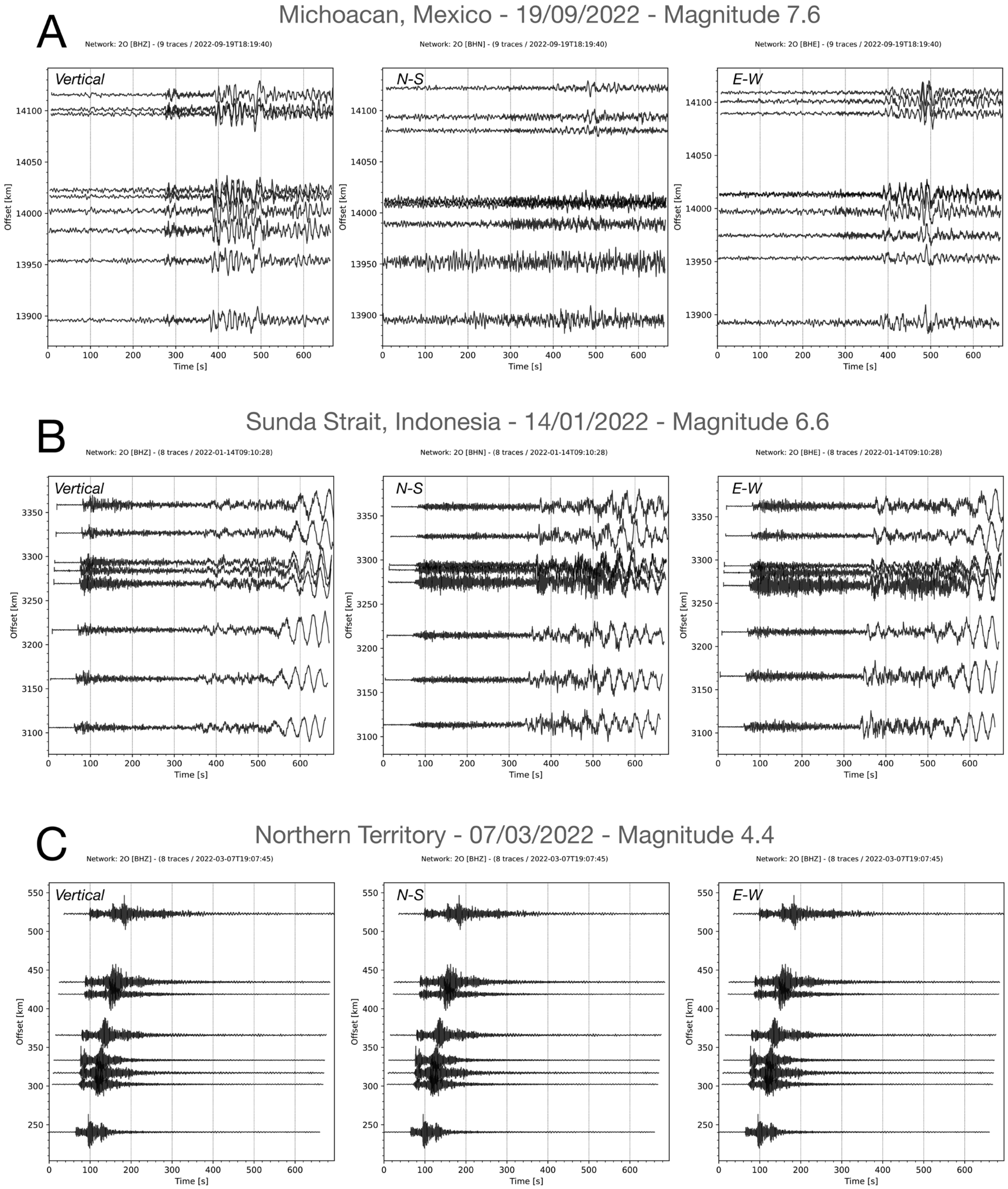

Figure 6: Three different earthquakes recorded by the Beetaloo Basin seismic network plotted for three components of the seismic sensor: vertical, north-south and east-west. The y-axis of each plot shows the distance between the earthquake and the station. A) Magnitude 7.7 Mexico earthquake. B) Magnitude 6.6 Sunda Strait, Indonesia earthquake. C) Magnitude 4.4 Northern Territory earthquake. Both the near and far-field earthquakes are clearly recorded by the seismic stations, showing the robustness of the sensors.

Baseline Seismic Detection & Location

Despite being one of the quietest zones in Australia (Figure 7), seismic activity does occur in the NT. For example, on January 22, 1988, three large earthquakes with magnitudes (Mw) 6.6, 6.3, 6.2 occurred within hours of each other in Tennant Creek, south of the Beetaloo Basin, and caused destruction. The aftershock activity of these events still continues today (Figure 8) following the expected pattern of reduced frequency and magnitude, typically conforming to a power law relationship known as Omori's law. Omori's law describes the decay of seismicity rate over time (Shearer, 2009).

However, the rest of the territory is relatively quiet, especially within the Beetaloo Basin.

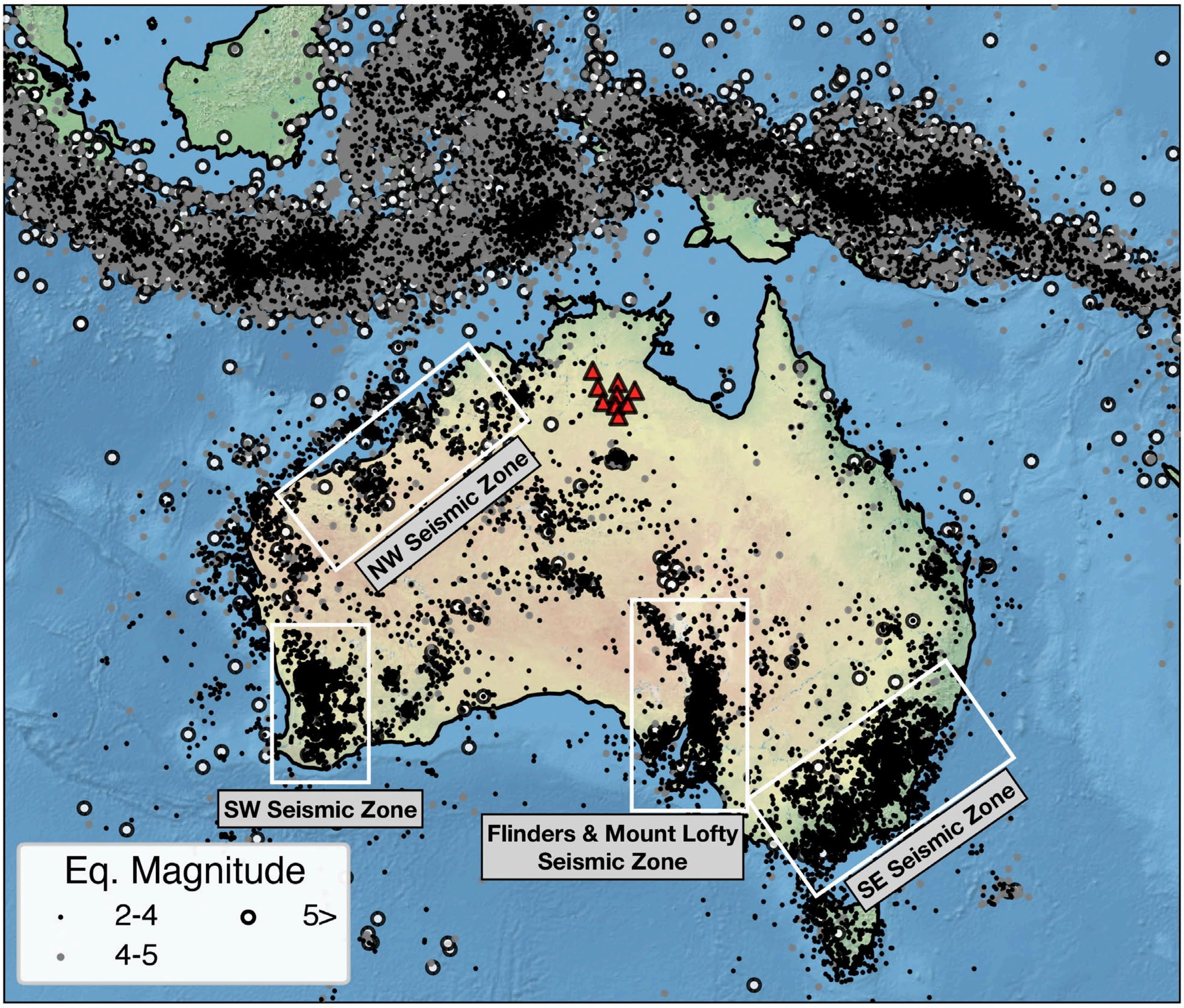

Figure 7: The distribution of earthquakes between 1900 and 2021 with magnitudes larger than 2 across the Australian continent. Four seismic zones are marked on the map. Modified from Rajabi et al. 2017. Source of the earthquakes: Geoscience Australia. Red triangles indicate the location of Beetaloo Seismic Network.

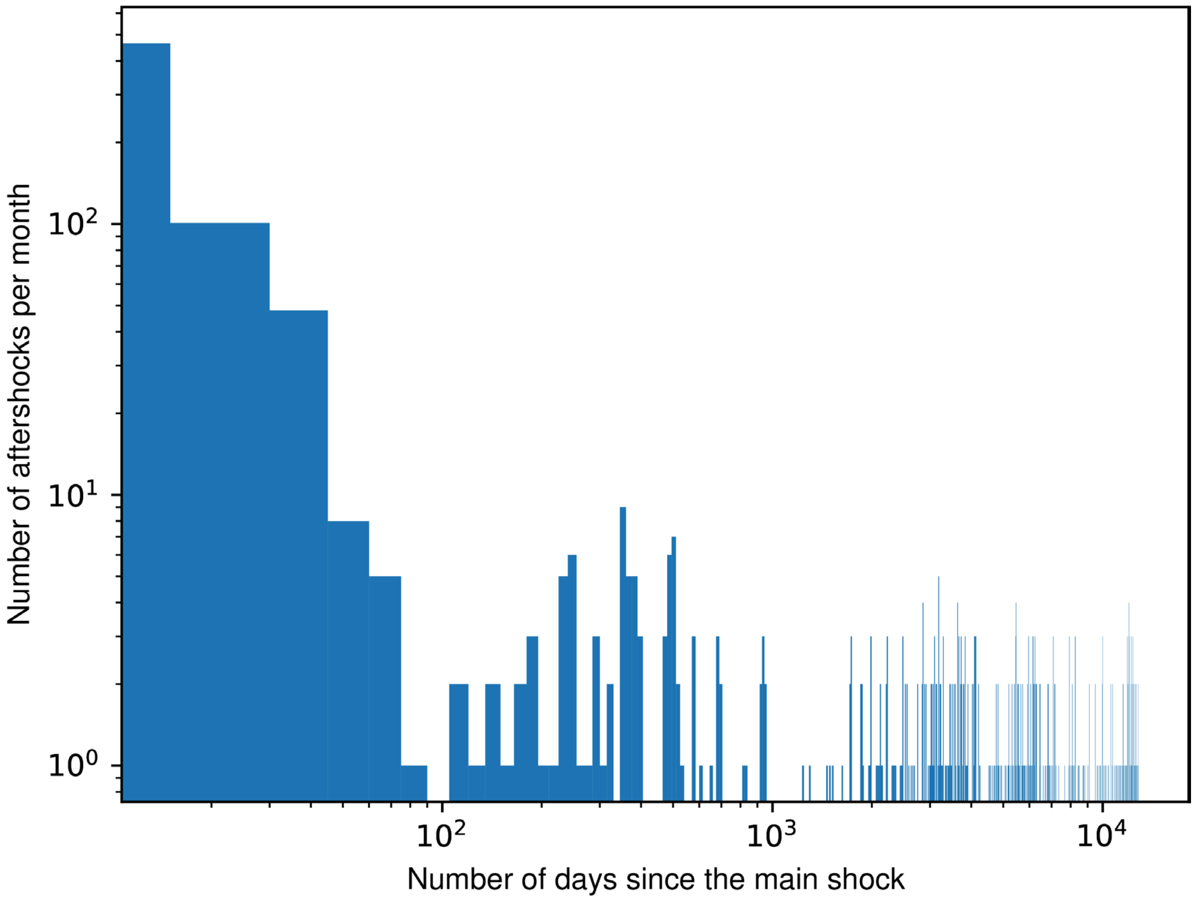

Figure 8 The aftershock distribution of 1988 Tennant Creek earthquakes. The distribution of the aftershocks shows a clear decay as expected following the Omori's Law. It is expected that the aftershocks will continue for another several decades.

We utilised the machine learning-based seismic detection algorithm developed by Mousavi et al. (2020) to analyse continuously recorded seismic data throughout December 2022. Through this analysis, we successfully identified more than 10 potential microseismic events exhibiting diverse seismic signal patterns. Figures 9-11 present plots of a subset of these events. Overall, the recorded signals demonstrate relatively weak yet coherent characteristics across multiple elements of the network for each event. The timing of these events suggests that their source cannot be attributed to anthropogenic activities, such as mining blasting, as most of them occurred later in the day. To further validate our findings, we cross-referenced the earthquake catalogues of both Geoscience Australia and USGS, but these events were not captured within their records.

The precise locations of these events, as well as future detections, will be determined in the subsequent stages of the project, following the complete integration of the seismic velocity model into the workflow.

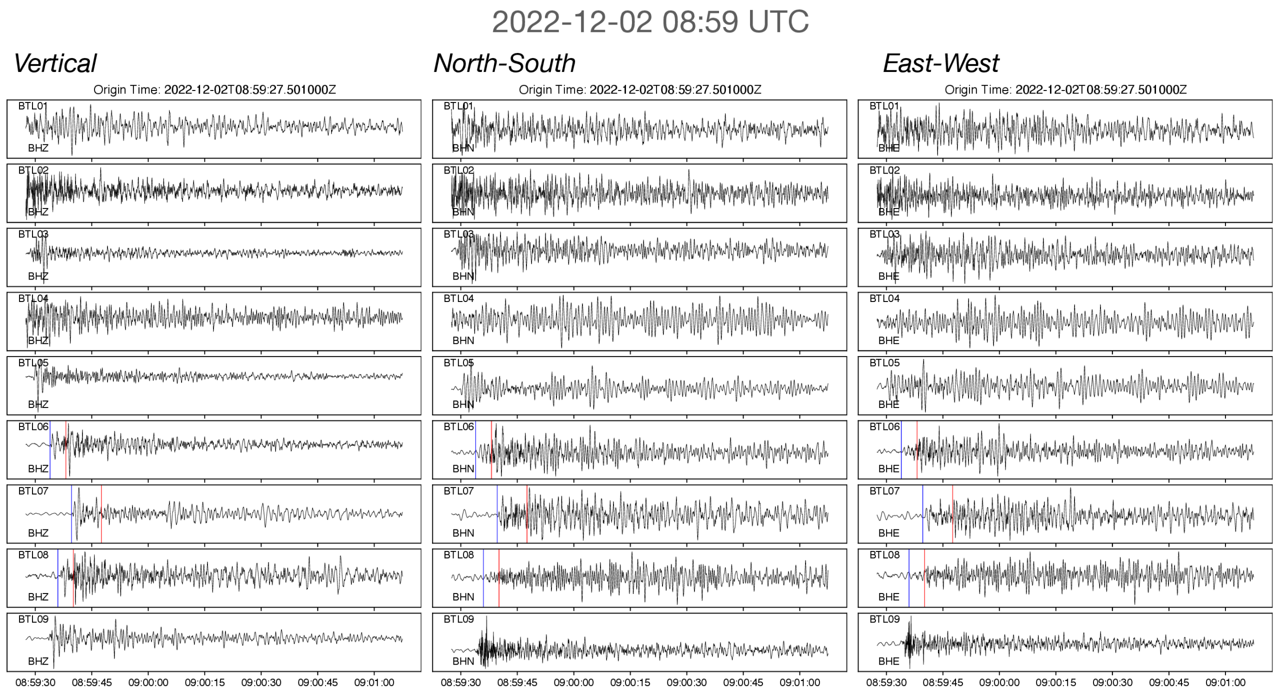

Figure 9: Example of earthquake detection on December 2, 2022. The coherence of waveforms and relative arrival differences at each station indicate a local/regional earthquake. The waveforms were filtered using a zero-phase Butterworth filter with a bandpass of 0.5-5 Hz.

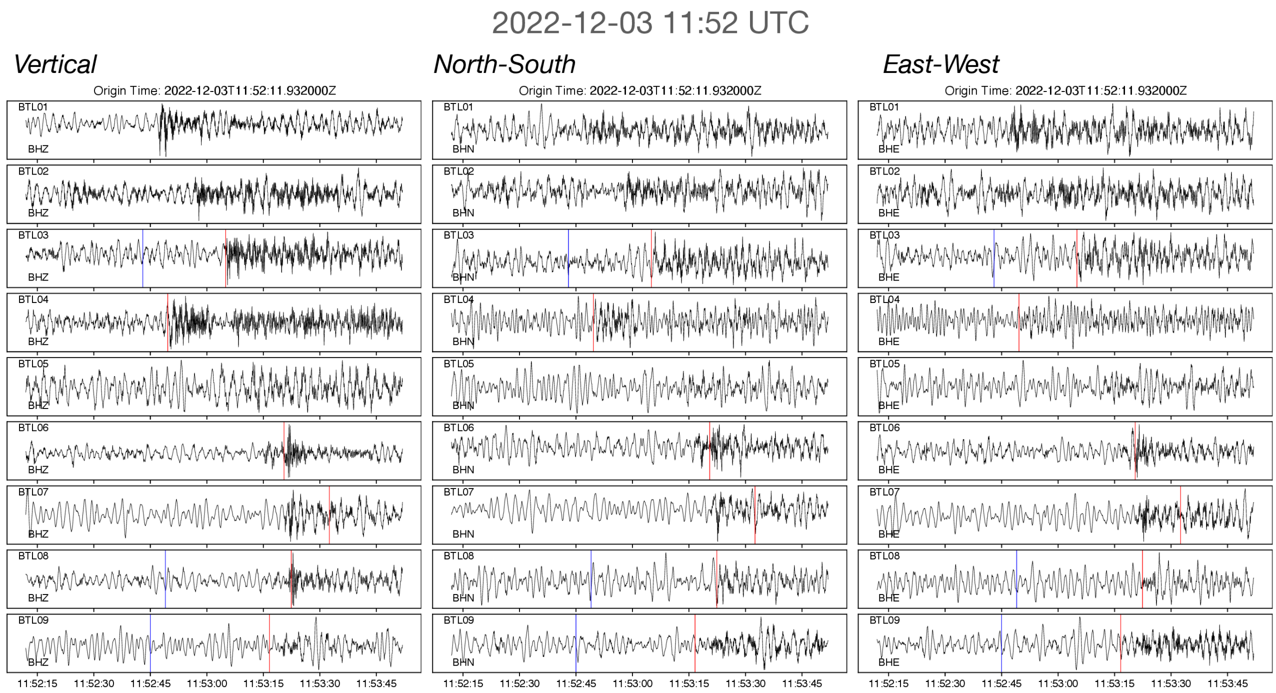

Figure 10: Example of earthquake detection on December 3, 2022. The coherence of waveforms and relative arrival differences at each station indicate a local/regional earthquake. The waveforms were filtered using a zero-phase Butterworth filter with a bandpass of 0.5-5 Hz.

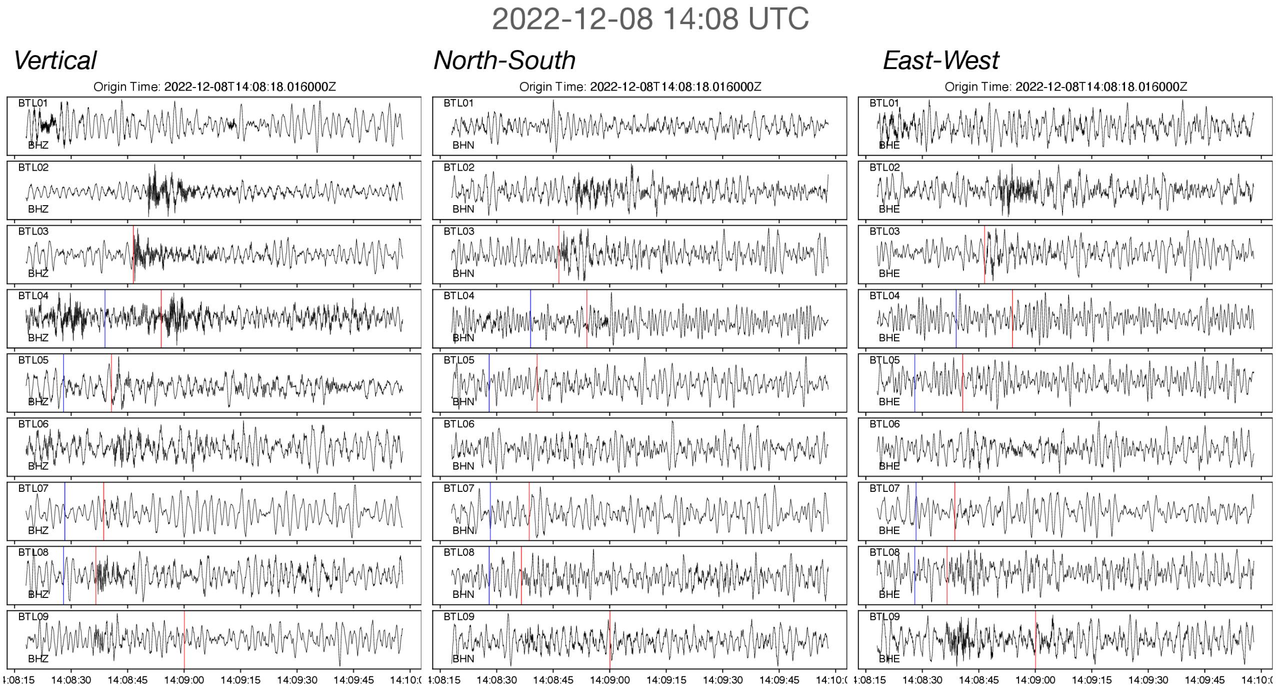

Figure 11: Example of earthquake detection on December 8, 2022. The coherence of waveforms and relative arrival differences at each station indicate a local/regional earthquake. The waveforms were filtered using a zero-phase Butterworth filter with a bandpass of 0.5-5 Hz.

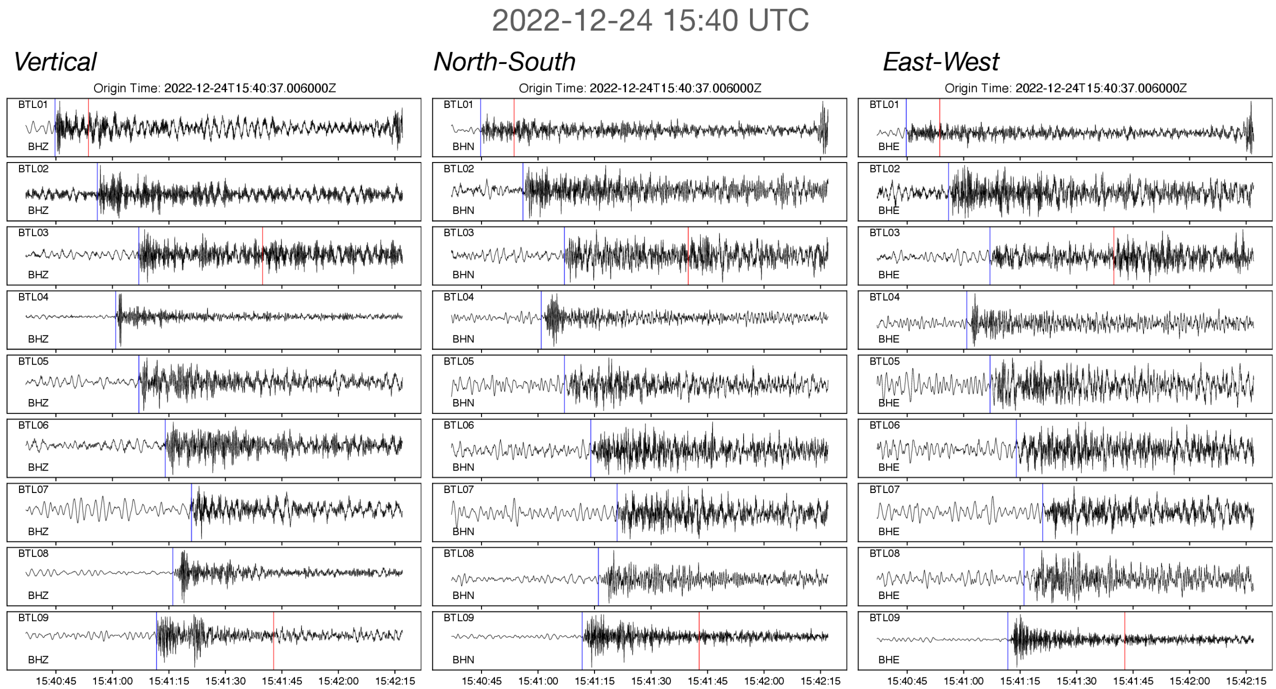

Figure 12: Example of earthquake detection on December 24, 2022. The coherence of waveforms and relative arrival differences at each station indicate a local/regional earthquake. The waveforms were filtered using a zero-phase Butterworth filter with a bandpass of 0.5-5 Hz.

Seismic Detection & Location

Seismic detection involves identifying earthquake signals from a range of non-earthquake signals and background noise recorded by a seismic sensor. Phase picking, on the other hand, refers to the process of identifying the arrival times of distinct seismic phases, such as the P-wave and S-wave, within an earthquake signal. These phases contain information about an earthquake and are used to determine its location.

We use a deep-learning workflow by Zhu & Beroza (2019) and Mousavi et al. (2020) for the simultaneous detection of earthquake signals and picking of P and S phases of the detected signals. This model is highly efficient in detecting and characterising smaller and more seismic events. The EQTransformer by Mousavi et al. (2020) generates results when at least one phase, either P or S, has a probability exceeding a user-defined threshold within a time window that has a high likelihood of representing an earthquake. Here, we used threshold values of 0.1, 0.01, and 0.01 for detection and P wave picking, and S wave-picking, respectively. We applied this workflow to all available data between 2019 and 2024 recorded by Geoscience Australia's Beetaloo Seismic Network (Glanville, 2019). For the velocity model, we used Chen et al. (2023), which is an Australia-wide seismic velocity model produced from seismic noise tomographic imaging previously by CSIRO scientists.

During this period, our workflow detected only four major events, all located in Glencore's McArthur River Mine (given in Table 1), which is approximately 200 km from the closest point of the array. These are large to very large mine blasts that have been properly registered by the network. Waveform plots for the vertical components of the events are given in Figures 13-16, and the location is shown in Figure 17. In Figure 17, we also show the yearly evolution of the array configuration, as some of stations were moved to increase the coverage. As the mine is quite far from the network, only very significant events were recorded. Although the outcome of this activity was not the intention of this study, these events show that the workflows are working as intended and are sensitive to seismicity as low as 2.29 and as far as 230 km from the centre of the array.

Event No	Origin Time (UTC)	Latitude (DD)	Longitude (DD)	Local Magnitude (Ml)
1	2022-04-04T05:04:46.121541Z	-16.601	136.248	2.75
2	2023-06-04T05:10:18.617616Z	-16.672	136.239	2.74
3	2023-11-13T05:25:57.708278Z	-16.288	136.195	2.40
4	2024-04-18T05:40:22.917387Z	-16.411	136.238	2.29

Table 1: Details of the detected seismic events between 2019 and 2024. All these signals originate from the McArthur River Mine during their large blasting activities. Note the similar origin time for each blast, which is between 14:30 and 15:10 local time.

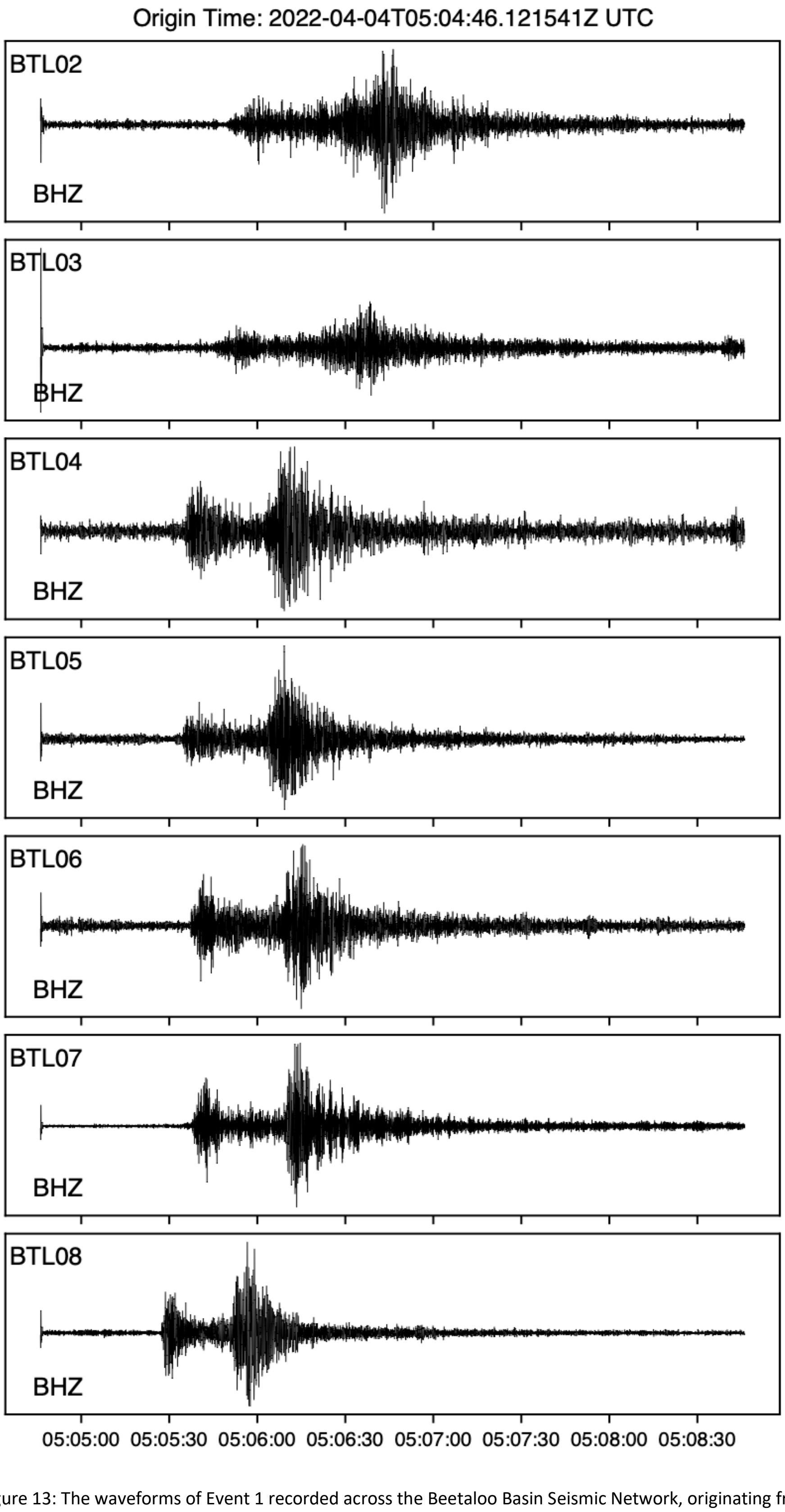

Figure 13: The waveforms of Event 1 recorded across the Beetaloo Basin Seismic Network, originating from the McArthur River Mine. Each waveform was filtered between 2 and 10 Hz, and the estimated local magnitude is 2.75.

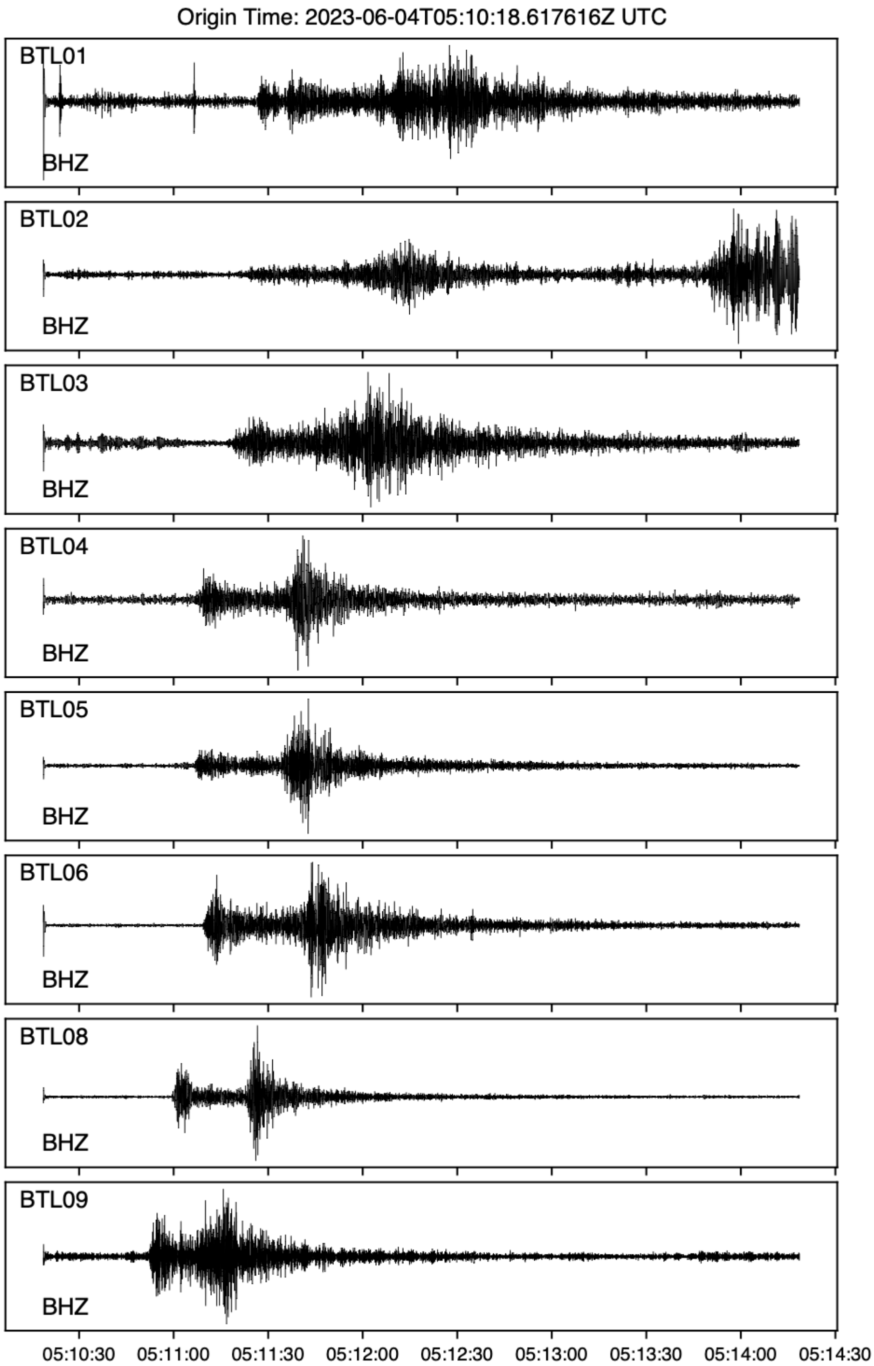

Figure 14: The waveforms of Event 2 recorded across the Beetaloo Basin Seismic Network, originating from the McArthur River Mine. Each waveform was filtered between 2 and 10 Hz, and the estimated local magnitude is 2.74.

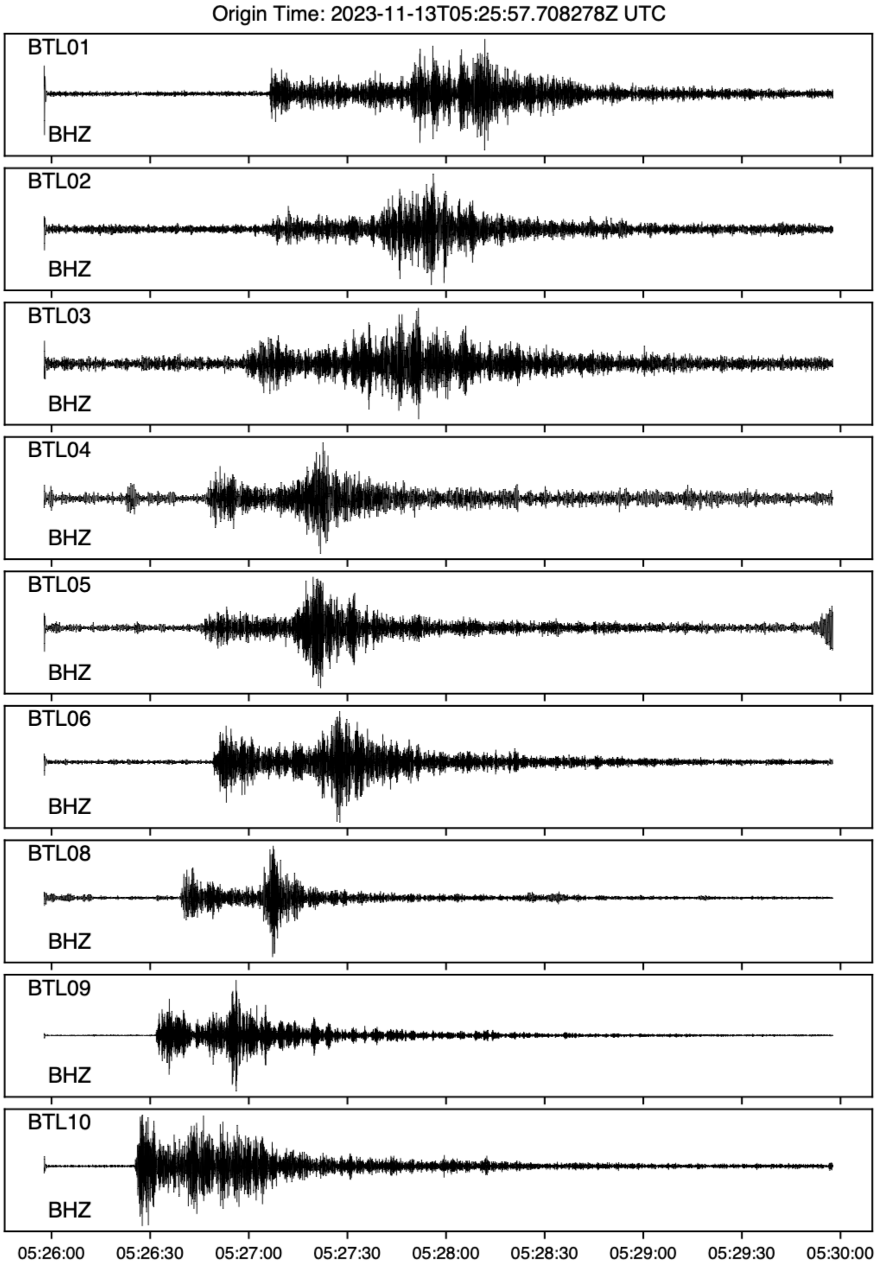

Figure 15: The waveforms of Event 3 recorded across the Beetaloo Basin Seismic Network, originating from the McArthur River Mine. Each waveform was filtered between 2 and 10 Hz, and the estimated local magnitude is 2.74.

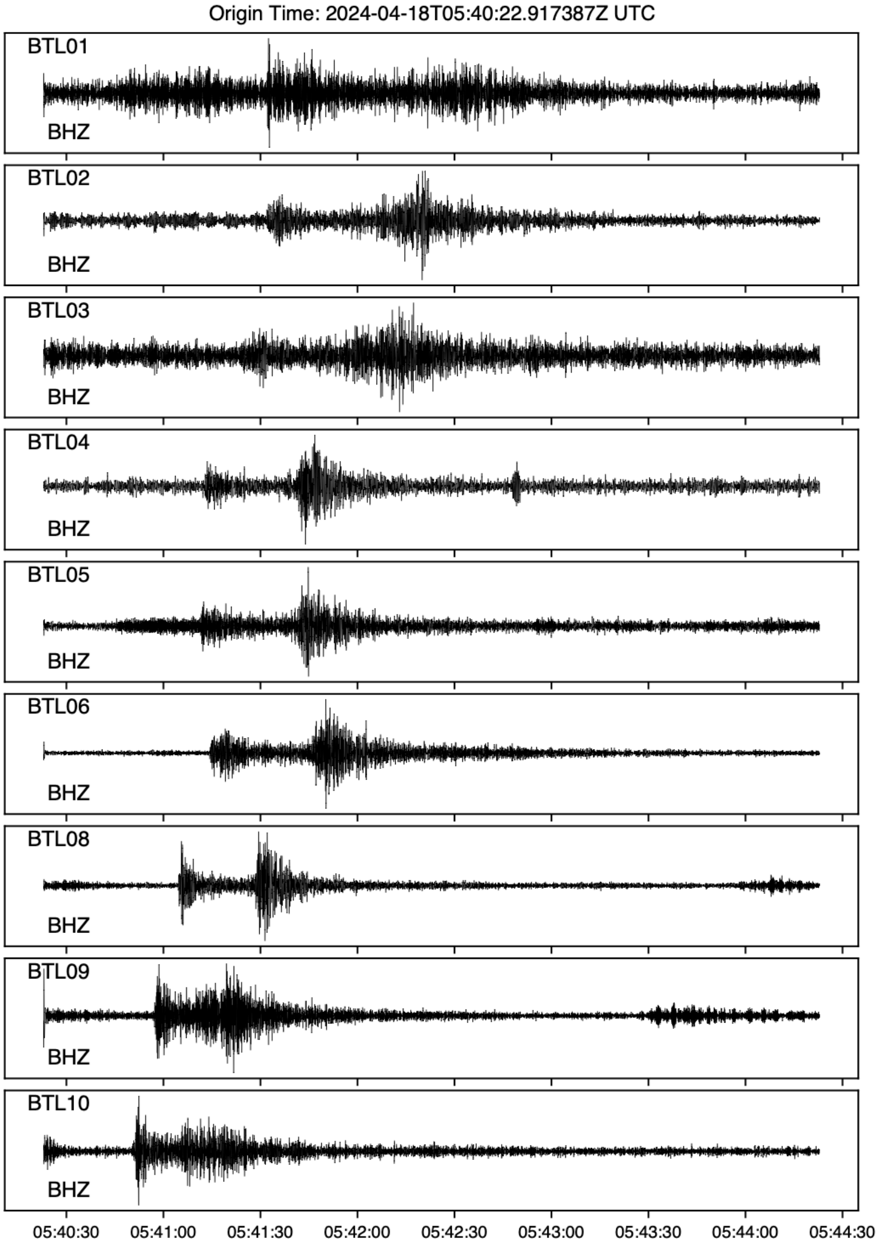

Figure 16: The waveforms of Event 4 recorded across the Beetaloo Basin Seismic Network, originating from the McArthur River Mine. Each waveform was filtered between 2 and 10 Hz, and the estimated local magnitude is 2.29.

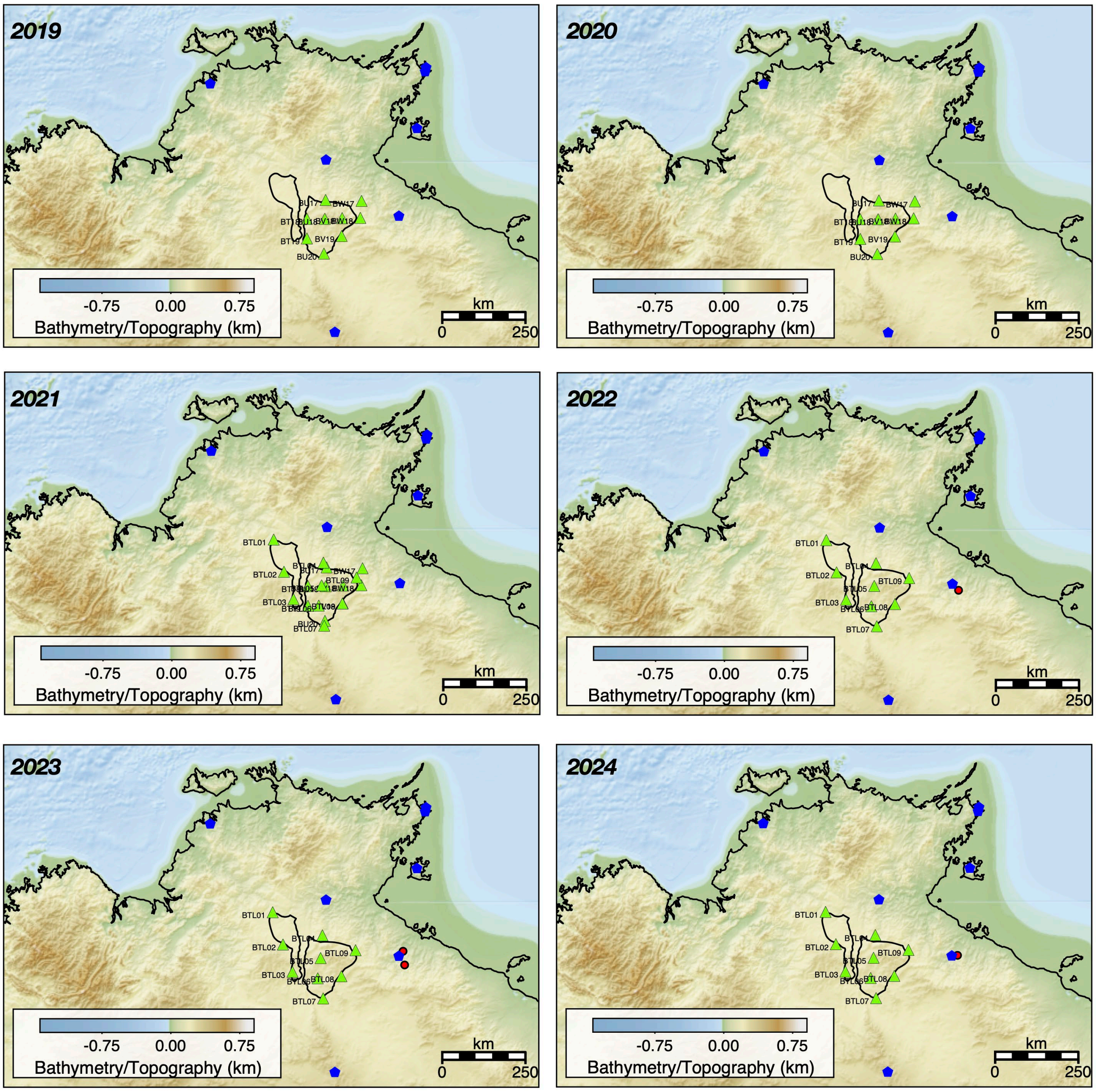

Figure 17: Yearly evolution of the Beetaloo Seismic array and also detected events between 2019 and 2024. The locations of the detected events are marked with red circles. Green triangles indicate the locations of the Beetaloo Seismic Network stations, and blue pentagons show the active mine sites. The McArthur River Mine is located near the red circles. The background topography and bathymetry are derived from ETOPO1 (Amante et al., 2009).

Ground Motion Simulations

Ground motion simulations are frequently utilized to assess the physical impacts induced by earthquakes over extensive distances. The presence of diverse geological structures, particularly sedimentary basins, can significantly influence wavefield propagation, frequency content, and amplitudes.

One common approach to quantifying the effect of earthquakes on infrastructure, such as buildings and residential areas, is to simulate wave propagation within the Earth for a hypothetical yet realistic earthquake scenario. In this study, we simulate the wave propagation for an earthquake with a magnitude of 5.1 that occurred on August 1, 2019, at 01:22:16 (UTC), approximately 300 km south of the Beetaloo Seismic array.

For the calculations, we utilized the Open-source Seismic Wave Propagation Code (OpenSWPC) package (Maeda et al., 2017). OpenSWPC is a 3D/2D finite-difference-based, full elastic waveform simulator. Our calculations were performed in 3D using a source wavelet with a dominant frequency of 0.25 Hz. The moment tensor parameters for the simulation were based on the parameters of the 2019 event. Given the computational complexity of computing 3D wavefield propagation across a large area, we employed high-performance computing by distributing the computations across 256 cores (4 nodes). The numerical simulation was performed at CSIRO's in-house Petrichor supercomputer, which took approximately 20 minutes. The grid size is 0.5 km in both the x and y directions, and is 0.1 km in depth. The time step is 0.01 s. For the 3D simulation, there were 1200 and 1400 grid points in the x and y direction, and 200 grid points in depth. As for the Earth model, we constructed a representative model using the recent work of Chen et al. (2023). This model incorporated shear wave velocities obtained through continent-wide ambient seismic noise tomography. For the P-wave velocities, scaling factors were applied. The spatial resolution of this model is approximately 1 degree, while the depth resolution is around 5 km. Among the nearby stations, BTL07 and BTL06 exhibited relatively high-amplitude arrivals, which aligns with expectations as the seismic energy experienced comparatively less attenuation. However, BTL05, located in the centre of the basin, demonstrated a sudden increase in amplitude. This observation is attributed to the slowing down of seismic waves in the sedimentary basins, leading to an amplification of seismic wave amplitudes. Conversely, BTL04, the furthest station from the simulated earthquake and outside the Beetaloo basin boundaries, exhibited the lowest amplitude (Figure 18 & Figure 19).

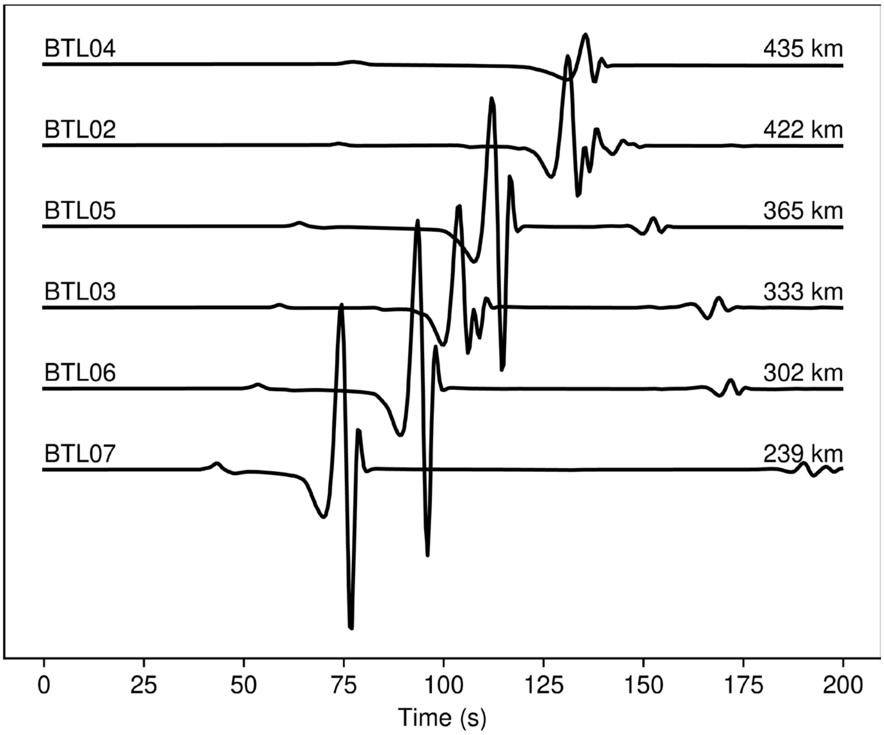

Figure 18 The simulated wavefield for the first 200 seconds of the 2019, 5.1 Tennant Creek earthquake. With increasing distance, more-complex wave trains can be observed across the network.

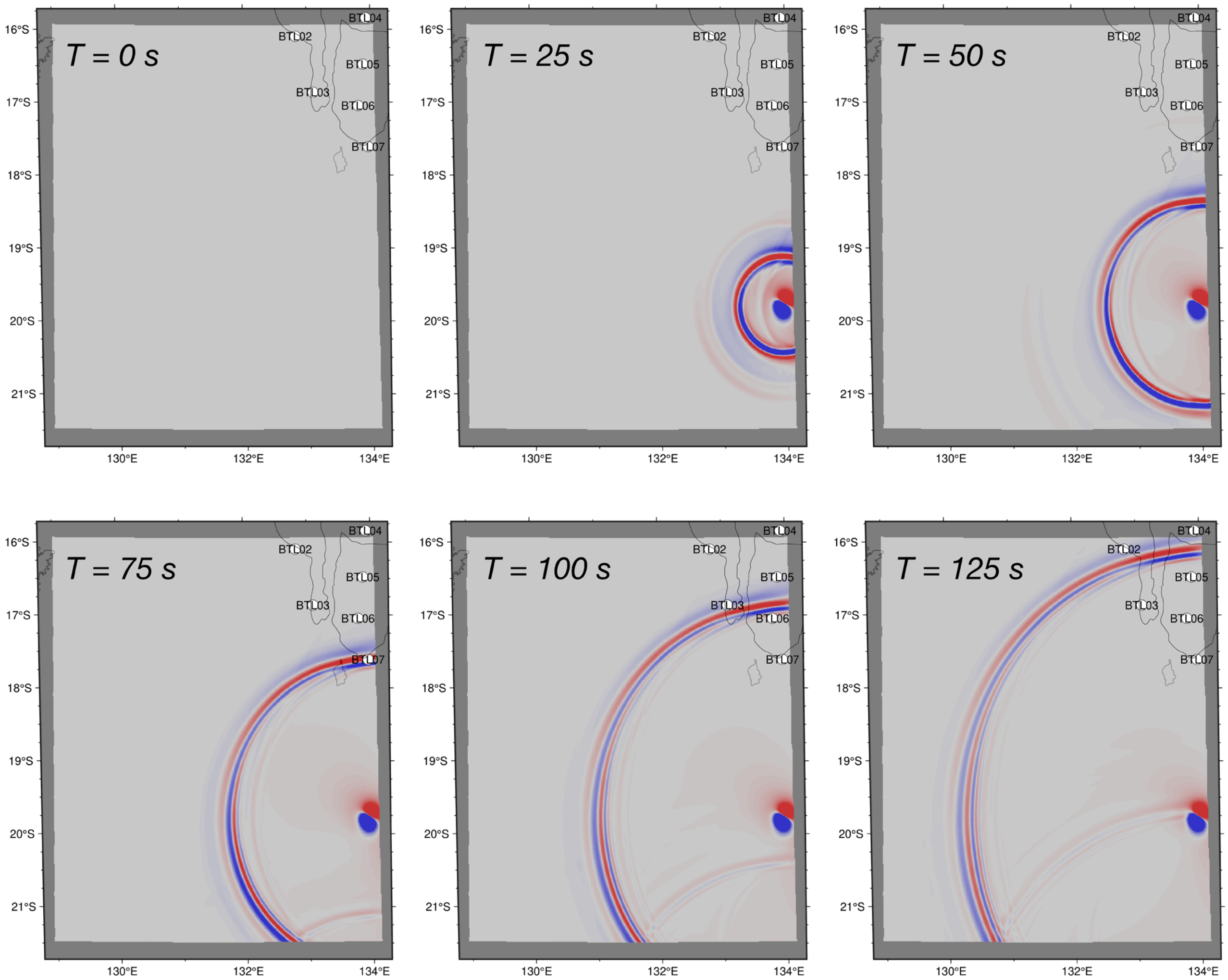

Figure 19 Snapshots of the computed wavefield between 0 - 125 seconds.

Future Perspectives

Seismic Risk

Although, we did not detect any local seismicity within the Beetaloo Basin after analysing more two years of data, this does not completely rule out the potential earthquake risk in the region.

In large stable continental regions (SCR), where there is no to minimal tectonic activity is taking place, it is notoriously difficult to quantify the seismic risk. On the other hand, tectonically active regions produce moderate to large magnitude earthquakes frequent enough fundamental seismic parameters such as the recurrence intervals of large earthquakes and maximum credible earthquake can be estimated (Leonard & Clark, 2011).

In Figure 20, we plot the general directions of the plate motion (blue arrows), where Australian continent is subducting under Eurasian continent (Indonesia and surroundings). The general stress directions (red arrows) are also plotted, where there is minimal correspondence between two for Australia. In tectonically active regions there is always a fair bit of correspondence between two observations. However, in stable continental regions such as Australia, the correspondence is limited and also does not provide any inputs to the seismic risk quantification.

In Beetaloo Basin, we have no information about the previous seismic activity, as the historical catalogues do not list any events, and paleoseismic studies (fault scarp mapping) are limited in this region and have not identified any scarps except in the Tennant Creek region south of the basin (see neotectonics website of Geoscience Australia). In the following sections, we argue that by designing a densely located seismic array, we can completely study the region and study the background seismicity. We also propose that by using advanced image processing methods augmented with recently developed machine learning methods, we can study high resolution digital elevation models and scan for the undocumented fault scarp signatures. At the end, if the new array detects earthquakes albeit with smaller magnitude (M<2), and any detected paleoseismic records (fault scarp signatures), we can confidently study baseline seismicity of the region.

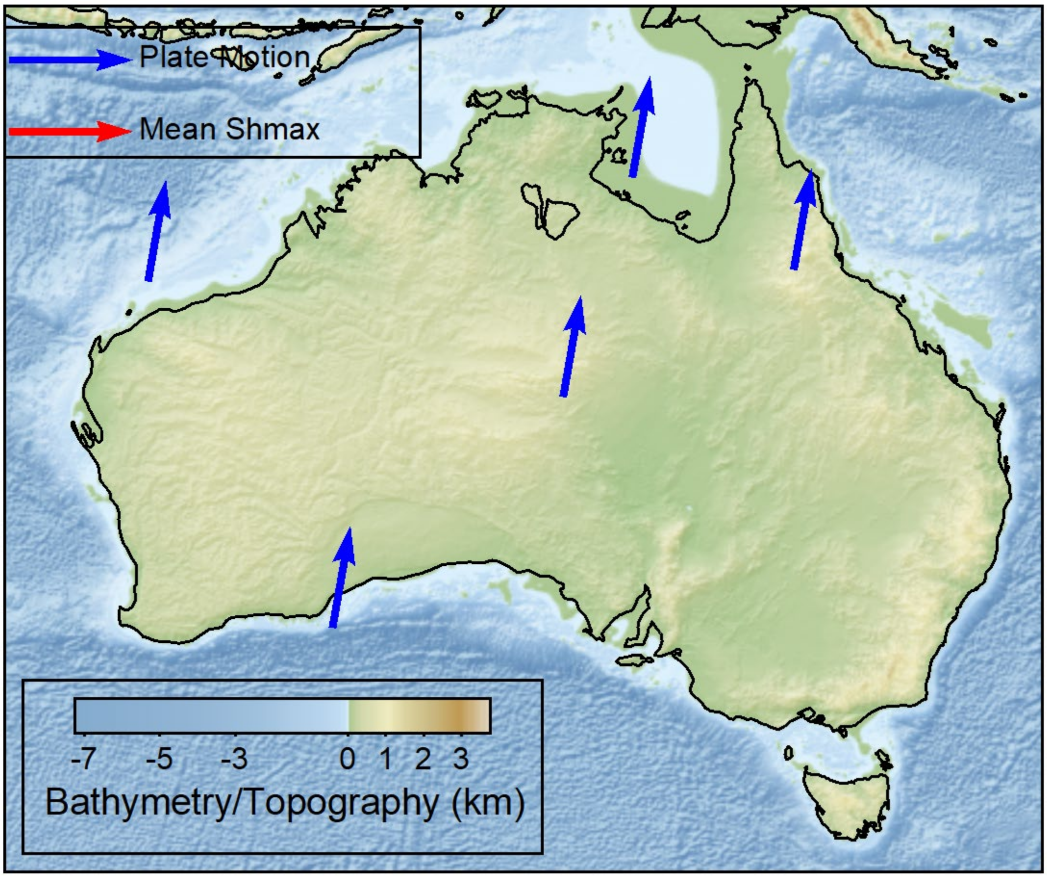

Figure 20 The general directions of the plate motion (blue arrows) are given, where Australian continent is subducting under Eurasian continent (Indonesia and surroundings). The general stress directions (red arrows) are also plotted, where there is minimal correspondence between two (source: Heidbach et al., 2018).

Optimum Seismic Network Design

The design of a seismic network is one of the most critical elements for the successful detection of seismic events. Often, seismologists use their professional intuition, logistical realities, and available instrumentation as key design parameters before deploying a seismic array for a specific purpose.

For (micro) seismic monitoring, prior knowledge of the expected locations of seismic events, local and regional geology, and environmental noise are also carefully considered.

Several previous studies have developed and applied optimal experimental design concepts to seismic network design. Kijko (1977) first developed the minimisation of the ellipsoid volume of earthquake location errors, also known as the “D-criterion”. Rabinowitz and Steinberg (1990) later expanded the D-optimal seismic network design method for multiple earthquakes and stations. This method relies on preselected hypothetical locations of earthquakes with different magnitudes and then uses an optimisation method to distribute the seismic stations to minimise location and depth uncertainty. Following this study, Hardt and Scherbaum (1994) used a simulated annealing approach to solve the optimisation problem for a selected 1D seismic velocity model. A subsequent study by Kraft et al. (2013) extended the Hardt and Scherbaum (1994) method and applied it to northern Switzerland for a large-scale microseismic monitoring network. They accounted for the influence of the seismic velocity model, ambient seismic noise levels, and wave attenuation to quantitatively design a seismic network.

In this section, we use the same approach as Kraft et al. (2013) for the Beetaloo region, selecting 10 randomly distributed seismic events with magnitudes ranging from 0.1 to 1.9 to calculate optimum seismic network configurations. For a region similar in size to the Beetaloo Basin, the detection of low-magnitude events requires densely clustered seismic stations, as can be seen in Figure 21, with a typical station spacing of less than 10 km.

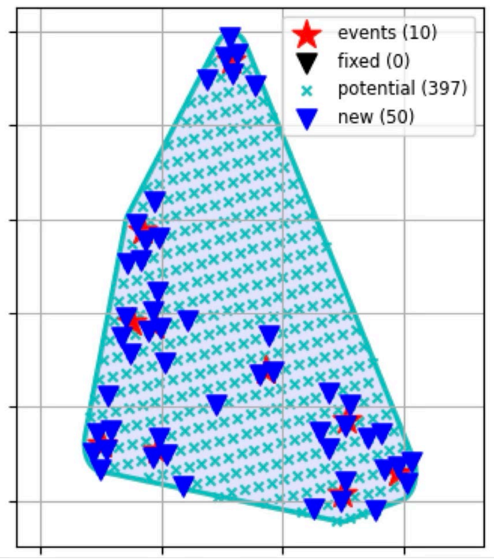

Figure 21 The distribution of hypothetical earthquakes (red stars) and location of clusters of seismic stations (blue inverted triangles). In x direction, each tick spacing corresponds to ~110 km, and in y-direction the tick spacing is ~55 km.

Neotectonic Studies

Fault scarps are often generated by large magnitude earthquakes (M > 6) and can be referred to as the surface imprint left by the tearing of the large earthquake (see Figure 22 for an example from the US). The preservation of the fault scarp on Earth is a function of the erosion rate, following seismic activity and urbanisation. In Australia, generally lower erosion rates, low population density, and sporadic seismic activity have led to the identification of several of these. Over the years, Geoscience Australia scientists have compiled a large collection of fault scarp information across the continent by conducting paleoseismic trenching and manually identifying these features by inspecting digital elevation images derived from SRTM90 data.

Figure 22 Fault scarp of 1983 Borah Peak earthquake, central Idaho, western United States. The magnitude of the earthquake was 6.9 and created extensive surface faulting (image credit: USGS)

Estimates from cosmogenic erosion rates (Quigley et al., 2007; King et al., 2019) suggest a 0.2 m scarp height could be removed within 20,000 – 40,000 years. Therefore, it is important to study these features systematically, as they provide clues about past seismicity, especially prior to the seismic instrumentation period (> 100 years).

Despite Geoscience Australia studying these features exhaustively and systematically, the manual process makes it cumbersome to study large areas. Here, we propose to borrow some tools from the machine learning community to identify and locate these features in the Northern Territory. Vega-Ramírez et al. (2021) showed that it is possible to use a machine learning-based algorithm to successfully detect fault scarp features in offshore domains. A similar workflow can be designed and readily applied to digital elevation datasets available for Australia. Training data can be sourced from the existing Neotectonic Database of Geoscience Australia.

Summary

In this project, we first assessed potential environmental noise sources in the region that could impact the detection performance of the seismic network. We then examined the seasonal variations in noise levels across the network, which showed minimal changes, with overall seismic noise levels remaining below the high noise model.

Utilising a machine learning-based detector, we used all available seismic data from the Beetaloo Seismic Network, deployed and operated by Geoscience Australia, to detect and document local seismic activity within the basin. During the analysis period between 2019 and 2024, in addition to the inconclusive detection of weak seismic signals (reported in the first interim report), we only detected major mining blasting activity coming from the east of the network, approximately 230 km from the centre of the network. We also integrated a recently developed 3D seismic-velocity model (Chen et al., 2023) into our 3D waveform simulations to evaluate the influence of geological structure on expected natural seismicity.

The 'lack' of detected seismic activity within the basin should be interpreted in light of the network sensitivity, where small magnitude earthquakes (e.g., Ml < 1) will not be registered due to background noise levels. With increasing distance, it becomes harder to differentiate signal from noise because of attenuation. Additionally, the nature of intraplate seismicity observed across Australia is aperiodic and separated by very long quiet periods of several tens of thousands of years.

In the final section of this report, we showed an example of optimum network design that has the potential to detect and locate events with magnitudes as low as 0.1. We also propose a machine learning-based method to automatically detect surface ruptures from past large earthquakes to quantify the probabilities of recurrence rates.

References

Amante, C., & Eakins, B. W. (2009). ETOPO1 arc-minute global relief model: procedures, data sources and analysis.

Chen, Y., Saygin, E., Kennett, B., Qashqai, M. T., Hauser, J., Lumley, D., & Sandiford, M. (2023). Next-generation seismic model of the Australian crust from synchronous and asynchronous ambient noise imaging. Nature Communications, 14(1), 1192.

Crone, A. J., Machette, M. N., & Bowman, J. R. (1993). *Geologic Investigations of the 1988 Tennant Creek, Australia, Earthquakes--Implications for Paleoseismicity in Stable Continental Regions: Investigations of the Paleoseismology, Deformation, and Quaternary Stratigraphy Associated with Reverse Faulting Caused by Three Major Earthquakes in the Interior of the Australian Craton* (No. 2032). US Government Printing Office.

Geoscience Australia. (n.d.). Neotectonic features. Geoscience Australia. https://neotectonics.ga.gov.au

Glanville, H. (2019). *Beetaloo Seismic Monitoring Project* [Data set]. International Federation of Digital Seismograph Networks. https://doi.org/10.7914/SN/2O_2019

Hardt, M., & Scherbaum, F. (1994). The design of optimum networks for aftershock recordings. *Geophysical Journal International*, *117*(3), 716-726.

Heidbach, O., Rajabi, M., Cui, X., Fuchs, K., Müller, B., Reinecker, J., ... & Zoback, M. (2018). The World Stress Map database release 2016: Crustal stress pattern across scales. *Tectonophysics*, *744*, 484-498.

Kennett, B. L. N. (2001). The seismic wavefield: Volume 1, Introduction and Theoretical Development (Vol. 1). Cambridge University Press.

Kijko, A. (1977). An algorithm for the optimum distribution of a regional seismic network—I. *Pure and applied geophysics*, *115*, 999-1009.

King, T., Quigley, M., Clark, D., Valkaniotis, S. N., Mohammadi, H., & Barnhart, W. D. (2019). The 1987 to 2019 Tennant Creek, Australia, earthquake sequence: A protracted intraplate multi-mainshock sequence (preprint).

Kraft, T., Mignan, A., & Giardini, D. (2013). Optimization of a large-scale microseismic monitoring network in northern Switzerland. *Geophysical Journal International*, *195*(1), 474-490.

Leonard, M., & Clark, D. (2011). A record of stable continental region earthquakes from Western Australia spanning the late Pleistocene: Insights for contemporary seismicity. *Earth and Planetary Science Letters*, *309*(3-4), 207-212.

Maeda, T., Takemura, S., & Furumura, T. (2017). OpenSWPC: an open-source integrated parallel simulation code for modeling seismic wave propagation in 3D heterogeneous viscoelastic media (Vol. 69, pp. 1-20). Springer Berlin Heidelberg.

Mousavi, S. M., Ellsworth, W. L., Zhu, W., Chuang, L. Y., & Beroza, G. C. (2020). Earthquake transformer—an attentive deep-learning model for simultaneous earthquake detection and phase picking. Nature communications, 11(1), 3952. McNamara, D. E., & Buland, R. P. (2004).

Ambient noise levels in the continental United States. Bulletin of the seismological society of America, 94(4), 1517-1527.

Quigley, M., Sandiford, M., Fifield, L. K., & Alimanovic, A. (2007). Landscape responses to intraplate tectonism: Quantitative constraints from 10Be nuclide abundances. *Earth and Planetary Science Letters*, *261*(1-2), 120-133.

Rabinowitz, N., & Steinberg, D. M. (1990). Optimal configuration of a seismographic network: a statistical approach. *Bulletin of the Seismological Society of America*, *80*(1), 187-196.

Rajabi, M., Tingay, M., Heidbach, O., Hillis, R., & Reynolds, S. (2017). The present-day stress field of Australia. Earth-Science Reviews, 168, 165-189.

Reading, A. M., Koper, K. D., Gal, M., Graham, L. S., Tkalčić, H., & Hemer, M. A. (2014). Dominant seismic noise sources in the Southern Ocean and West Pacific, 2000–2012, recorded at the Warramunga Seismic Array, Australia. Geophysical Research Letters, *41*(10), 3455-3463.

Shamsalsadati S. Allen T. Çomoğlu M., and Glanville H. (2021). The Beetaloo sub-basin baseline seismic monitoring project—Phase 1 observations, Australian Earthquake Engineering Society 2021 Virtual Conference.

Shearer, P. M. (2009). Introduction to seismology. Cambridge University Press.

Vega-Ramírez, L. A., Spelz, R. M., Negrete-Aranda, R., Neumann, F., Caress, D. W., Clague, D. A., ... & Peña-Dominguez, J. G. (2021). A new method for fault-scarp detection using linear discriminant analysis in high-resolution bathymetry data from the Alarcón rise and Pescadero basin. Tectonics, 40(12), e2021TC006925.

Zhu, W., & Beroza, G. C. (2019). PhaseNet: a deep-neural-network-based seismic arrival-time picking method. *Geophysical Journal International*, *216*(1), 261-273.

As Australia's national science agency and innovation catalyst, CSIRO is solving the greatest challenges through innovative science and technology.

CSIRO. Unlocking a better future for everyone.

Contact us

1300 363 400
+61 3 9545 2176
csiro.au

For further information

1300 363 400
gisera.csiro.au

GISERA is a collaboration between CSIRO, Commonwealth and state governments and industry established to undertake publicly-reported independent research. The purpose of GISERA is to provide quality assured scientific research and information to communities living in gas development regions focusing on social and environmental topics including: groundwater and surface water, greenhouse gas emissions, biodiversity, land management, the marine environment, and socio-economic impacts. The governance structure for GISERA is designed to provide for and protect research independence and transparency of research.